Pediatr Cardiol 21:70–79, 2000
DOI: 10.1007/s002469910009

Pediatric Cardiology

Clinical Applications of Cardiac Magnetic Resonance Imaging After Repair of Tetralogy of Fallot

W.A. Helbing,[1] **A. de Roos**[2]

[1]Department of Pediatrics, Division of Pediatric Cardiology, Leiden University Medical Center, J-6-S, P.O. Box 9600, 2300 RC Leiden, The Netherlands

[2]Department of Radiology, Leiden University Medical Center, J-6-S, P.O. Box 9600, 2300 RC Leiden, The Netherlands

Abstract. In the past 15 years, cardiovascular magnetic resonance (MR) has evolved into an imaging technique that provides adequate, and in part unique, information on residual problems in the follow-up of patients operated for tetralogy of Fallot. Spin-echo or gradient-echo cine magnetic resonance imaging allow detailed assessment of intracardiac and large vessel anatomy, which is particularly helpful in Fallot patients with residual abnormalities of right ventricular outflow and/or pulmonary artery. Multisection gradient-echo cine MRI can be used to obtain accurate measurements of biventricular size, ejection fraction, and wall mass. This allows serial follow-up of biventricular function. MR velocity mapping is the only imaging technique available that provides practical quantification of pulmonary regurgitation volume. MR velocity mapping can also be used to quantify right ventricular diastolic function in the presence of pulmonary regurgitation.

Key words: Magnetic resonance imaging — Pulmonary regurgitation — Restrictive diastolic physiology — Tetralogy of Fallot — Ventricular function — Ventricular hypertrophy

Tetralogy of Fallot (TOF) is the most common type of cyanotic congenital heart disease. Its incidence is approximately 5% or 6% of all patients with congenital heart disease [31]. Since the introduction of total surgical repair in 1955 [44], the long-term prognosis for these patients has become good but less than that of the normal age-matched population [57, 63]. Total repair within the first months of life is currently feasible [73], with low mortality. However, complications, residua, and sequelae may result in problems after total repair of TOF.

In the follow-up of patients who have undergone repair of TOF an imaging technique is required that provides adequate information on (1) residual anatomical problems [ventricular septal defect (VSD), pulmonary stenosis, and right ventricular (RV) outflow aneurysm], (2) the extent of pulmonary stenosis (residual or recurrent), (3) the amount of pulmonary regurgitation, and (4) systolic and diastolic biventricular size and function. Echocardiography remains the principal diagnostic tool in these patients [22]. However, because of well-known limitations, transthoracic echocardiography often fails to provide necessary hemodynamic or anatomic information, particularly in operated patients [30, 48]. Magnetic resonance imaging (MRI) gives noninvasive images of the cardiovascular system with excellent image quality, unlimited choice of imaging planes, and accurate flow quantification, without the use of ionizing radiation. In the past 15 years, the role of MRI in cardiovascular imaging has gradually evolved. The purpose of this article is to review current clinical applications of MRI in patients operated for TOF.

MRI of Postoperative Anatomy

Six to 10% of patients after repair of TOF will require reoperation because of residual or recurrent VSD, RV outflow obstruction or aneurysm formation, and pulmonary artery stenosis [57, 63]. From the initial reports on the successful use of MRI for cardiovascular imaging, this technique has been recognized as well suited to image cardiac anatomy in postoperative patients with congenital heart disease, including those with TOF [10, 14, 15, 23, 27, 29, 36]. Both intracardiac and large vessel anatomy may be depicted clearly with electrocardiogram (ECG) gated spin-echo images [12, 38]. Transaxial, coronal, and sagittal views are generally applied. Angulated views tailored to the anatomical region of interest may provide additional information. Thus, RV hypertrophy, RV outflow tract stenosis, and pulmonary artery

Correspondence to: W.A. Helbing

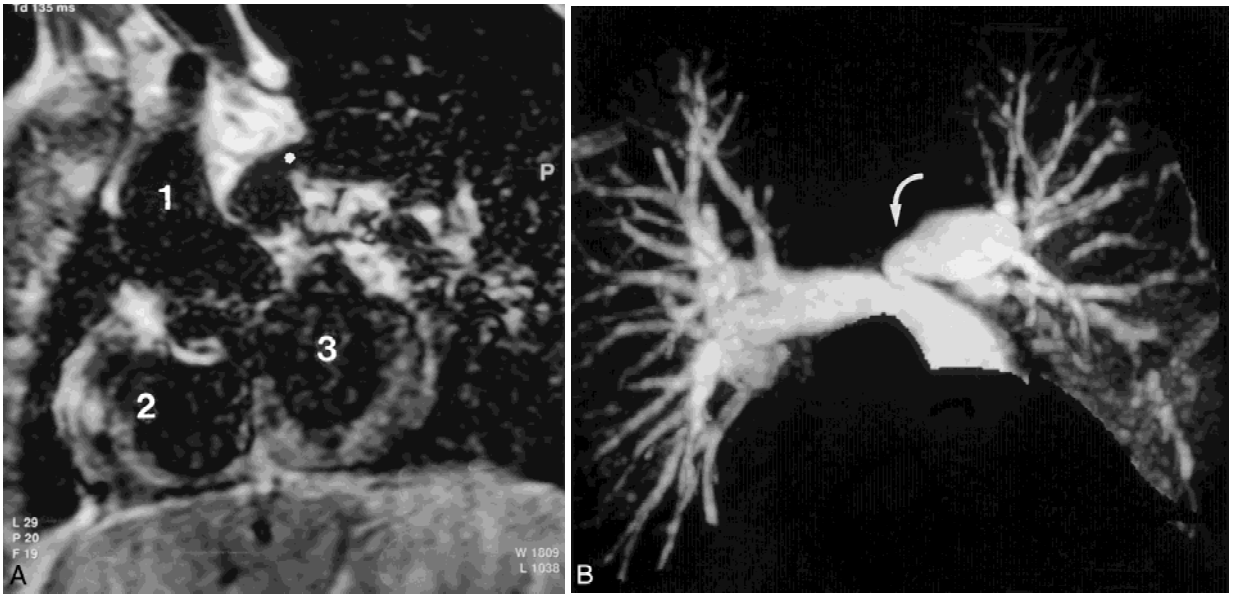

Fig. 1. (A) Spin-echo image (coronal plane) of pulmonary artery of patient after correction of tetralogy of Fallot. Narrowing of the proximal left pulmonary artery is indicated (*). *1*, aorta; *2*, right ventricle; *3*, left ventricle. **(B)** MIP projection of gadolinium-enhanced 3-D MR angiogram of pulmonary artery of same patient (Fig. 1A). Narrowing of the proximal left pulmonary artery is indicated (*arrow*). Note detailed imaging of pulmonary artery branches.

anatomy and size may be assessed in postoperative TOF patients [1, 12, 14, 28, 29, 52]. For evaluation of RV outflow, main pulmonary artery (PA), and (PA) branches, angiography has long been considered the "gold standard." Of the noninvasive techniques, spin-echo MRI and transthoracic echocardiography are equivalent for assessment of RV outflow and main PA in most patients, provided the acoustic window is adequate for echocardiography [12]. The sensitivity and specificity of these techniques are adequate for clinical purposes if compared with angiography [38, 87]. For identification of abnormalities of the left and right pulmonary artery, spin-echo MRI is clearly better than transthoracic echocardiography [12, 52, 91] (Fig. 1A). However, with non-contrast spin-echo MRI (2- and 3-dimensional), visualization of the peripheral pulmonary arteries is problematic, as is evaluation of the number and distribution of collateral vessels [28, 89, 90, 91]. Gradient-echo cine MR provides high contrast between lumens of blood vessels and adjacent tissues, rendering it an attractive technique for assessment of PA and aortopulmonary collateral vessel size and anatomy [91]. Contrast enhanced 3-D MR angiography is a relatively new technique that has allowed adequate visualization of thoracic large vessels [35, 42, 86]. The technique has successfully been applied in patients with congenital heart disease [42], but detailed evaluation in patients with TOF has not been performed (Fig. 1B).

Gradient-echo MRI allows the identification of a residual or recurrent VSD. Turbulent flow caused by the shunt through the VSD will result in proton dephasing within the jet. This will result in a local loss of signal intensity, observed as a signal void on gradient-echo images (Fig. 2). However, systematic evaluation of the use of MRI in the detection of residual VSDs has, to our knowledge, not been performed.

Many of the limitations of transthoracic echocardiography may be overcome by transesophageal echocardiography (TEE). In comparison to TEE, MRI provides better information on large vessel anatomy, including pulmonary artery branches [30]. For intracardiac anatomy and atrioventricular (AV) valve function TEE is probably better suited [30]. This allows a choice of imaging technique, tailored to the clinical problem.

Postoperative Functional Evaluation

Pulmonary Regurgitation

The current surgical policy in TOF, aimed at early complete surgical correction, results in considerable transannular patch rates, which induces residual pulmonary regurgitation [39]. Residual pulmonary regurgitation has been associated with RV dilatation, impaired biventricular function, limited exercise tolerance, and increased risk for ventricular arrhythmias [3, 70, 74, 77]. Therefore, assessment of the amount of pulmonary regurgitation is of direct clinical importance. Until recently, no practical, clinically useful technique for quantification of

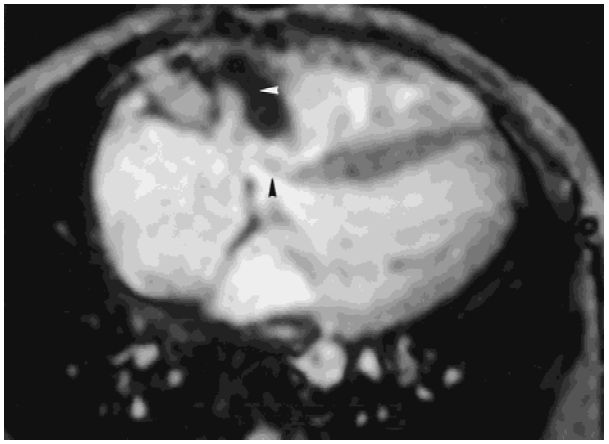

Fig. 2. Gradient-echo MR image (transverse plane) at ventricular level of patient after Fallot repair. Note the VSD patch (*black arrowhead*). Signal void (*white arrowhead*) indicates turbulent flow into the RV caused by shunt flow through a residual VSD.

pulmonary regurgitation was available despite attempts using many different methods, including Doppler echocardiography, contrast ventriculography, and videodensitometry [40, 49, 74].

Velocity mapping MR is an accurate technique to assess velocity and volume of flow [13, 51, 84]. MR velocity mapping allows noninvasive, accurate quantification of valvular regurgitation, including pulmonary regurgitation in TOF [70, 72]. Rebergen et al. [70] studied 18 patients after repair of TOF. Age at repair of these patients was 3.9 ± 2.4 years, and age at the MR study was 16.5 ± 6.5 years. A transannular patch was used at repair in 8 patients [70]. MR velocity mapping was performed in a double-oblique plane, perpendicular to the main PA just below the bifurcation. The cardiac cycle was sampled with a time frame of 30 msec; resulting in 16 to 28 time frames, depending on heart rate. Instantaneous flow volumes in the PA were calculated by multiplying PA contour area (traced manually) with the spatial average flow within this contour [70]. Total forward and regurgitant flow per heart cycle were calculated by summation of instantaneous flow volumes (Fig. 3). Pulmonary forward flow showed good correlation with RV stroke volume as derived from multisection, multiphase gradient-echo MRI in patients without tricuspid regurgitation. The agreement between velocity mapping measurements of pulmonary regurgitant volume and the difference between right versus left ventricular stroke volume as obtained with multisection cine MRI was excellent [70]. Pulmonary regurgitant volume index ranged from 0.21 to 4.23 L/min/m^2 (mean 1.47 ± 1.17 L/min/m^2; 30 ± 18% of RV stroke volume). Significant differences in the amount of pulmonary regurgitation could be observed between patients with and those without a transannular patch [70]. This study clearly demonstrated the feasibility of assessment of quantification of pulmonary regurgitation in TOF and has provided the basis for several other clinical studies in TOF patients [9, 25, 60]. Earlier studies, in which the amount of pulmonary regurgitation could not be quantified in a practical way, suggested a negative influence of the amount of pulmonary regurgitation on exercise performance [8, 49, 74, 76, 94]. In a study of 19 children (age 12 ± 3 years) we confirmed with MRI that the actual amount of pulmonary regurgitation correlates directly with exercise performance [59]. Singh et al. [85] had similar observations in a recent MRI study.

The main disadvantage of MRI measurements of pulmonary regurgitation is that beat to beat information cannot be obtained with current MRI techniques [9]. This has hampered evaluation of respiratory influences on the amount of pulmonary regurgitation [9].

Pulmonary Stenosis

Right ventricular outflow and PA stenosis are among the most common hemodynamic problems after repair of TOF [9, 57, 63]. Adequate evaluation of these problems requires proper identification of the location and extent of the stenosis. As previously discussed, MRI is an adequate technique to study the morphology of the RV outflow and pulmonary arteries. MR velocity mapping enables measurement of velocities across a stenotic area. Using the modified Bernoulli equation the stenotic gradient can be calculated. This technique does not differ from Doppler echocardiography in its practical applications. The main advantage of MR velocity mapping compared to Doppler echocardiography is the unlimited choice of imaging planes with MRI. This allows for alignment with the velocity jet in any direction, which is often difficult with Doppler echocardiography, particularly in branch pulmonary stenosis. Separate assessment of left and right PA flow has been performed with MR velocity mapping in healthy volunteers and patients after a Fontan operation [7, 71]. This technique could be used to assess lung perfusion in TOF patients with branch pulmonary stenosis, possibly predicting the need for relief of local stenoses with a stent or surgical procedure. To our knowledge, MR has not been used for this purpose in patients with TOF.

Function of the Right and Left Ventricle

The importance of RV function as a determinant of outcome after repair of TOF has been underlined by many studies [21, 33, 39, 74, 94]. The combined effects of preoperative hypertrophy and hypoxemia, operative factors, and residual postoperative problems as pulmonary regurgitation and/or stenosis may result in impaired RV

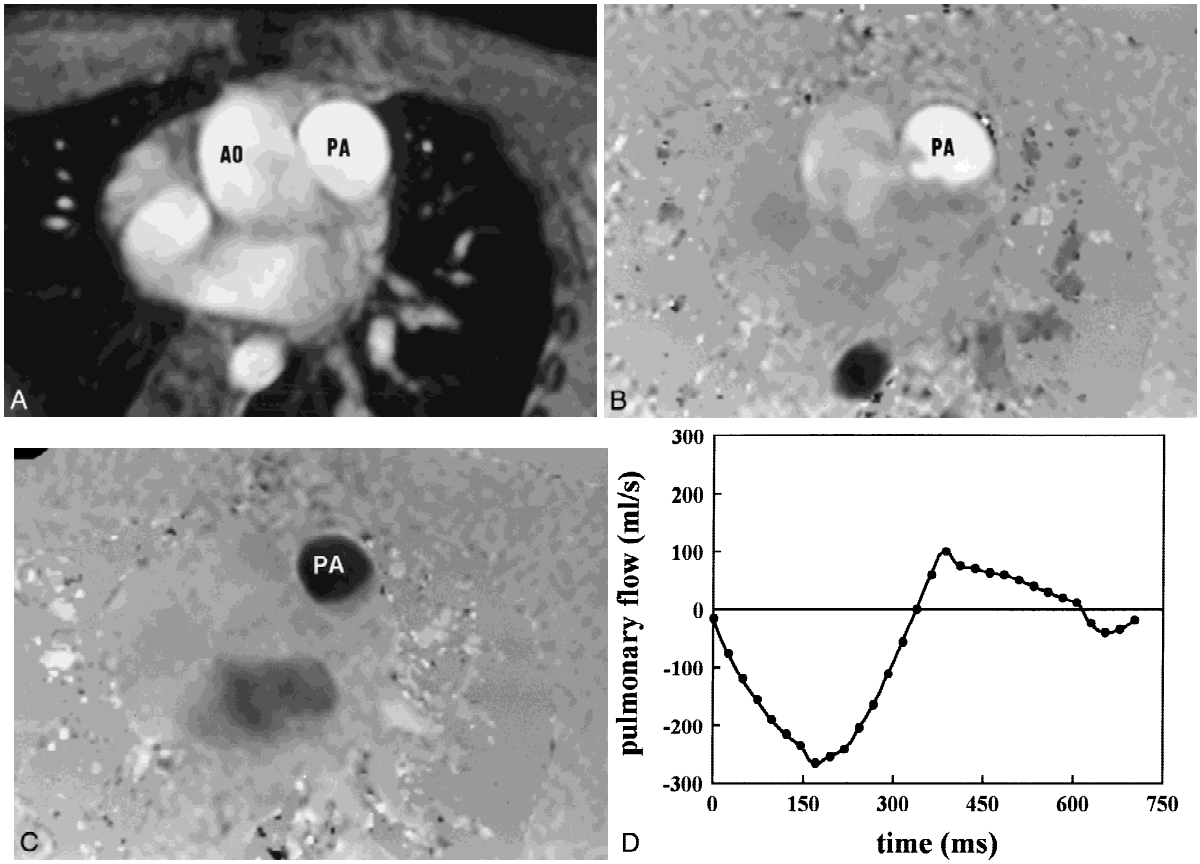

Fig. 3. (A) Double oblique magnitude image obtained with the flow-adjusted gradient across the main pulmonary artery (*PA*) in early systole. *AO*, aorta. **(B)** Velocity map corresponding to Fig. 3A. Bright signal indicates (systolic) flow out of the right ventricle. Spatial peak and spatial average velocities are obtained from the brightest and average signal intensities across the pulmonary artery lumen, which is manually outlined. *PA*, pulmonary artery. **(C)** Velocity map of the same patient as in Figs. 3A and 3B. Dark signal indicates (diastolic) flow back into the right ventricle. Spatial peak and spatial average velocities are obtained from the darkest and average signal intensities across the pulmonary artery lumen, which is manually outlined (*PA*). Note mid-gray signal intensity in ascending aorta, indicating stationary or zero flow velocity in this diastolic time frame. **(D)** Time–volume flow velocity curve of pulmonary artery. Flow velocity–time frame was calculated by multiplying pulmonary artery contour area (Figs. 3B and 3C; traced manually) with the spatial average flow within this contour. Negative values indicate flow out of the right ventricle. Note diastolic backward flow during most of diastole, indicating pulmonary regurgitation, and late diastolic forward flow at end diastole.

function [3, 32, 37, 47, 67, 74, 75, 93, 95]. Serial noninvasive assessment of RV function is therefore required during follow-up of these patients. In patients with adequate acoustic windows, qualitative or simple quantitative transthoracic 2-D echocardiographic methods to assess RV size and ejection fraction may be used to select those patients in whom further evaluation is required [24]. As a result of problems in obtaining maximal RV dimensions, difficulties in obtaining standardized views, and intrinsic inadequacies in geometrical assumptions of the complex RV shape, transthoracic echocardiography has limited value for accurate assessment of RV size and ejection fraction [24, 34, 41, 43, 61, 66, 83], particularly in the operated older child, adolescent, and adult. Three-dimensional echocardiography is a promising technique for measurement of RV size, but it has not been used for clinical studies in TOF [68, 92]. Multisection cine MRI provides dimensionally accurate RV volume measurements [4, 26, 45, 62], even with abnormal RV shape. This is particularly important in the follow-up of patients with abnormal RV loading conditions.

The advantages of MRI compared to other noninvasive imaging techniques are less clear for the left ventricle (LV). However, the shape of the LV is altered in RV volume overload states, as with pulmonary regurgitation after TOF repair [78]. In these situations, calculations that rely on the assumption of a normal LV shape may not be accurate. LV volumes may be assessed without assumptions of ventricular geometry with MRI. MRI also allows detailed analysis of changes in LV wall thickness during the cardiac cycle [6].

Potential limitations of the technique include the time-consuming nature of analysis of a multisection, multiphase data set. The coarse trabeculation of the RV

endocardium may hamper manual drawing of the endocardial border of the RV. Despite these problems, acceptable inter- and intraobserver variation for right and left ventricular volume measurements have been established [4, 26, 62].

Particularly for RV measurements, consensus with regard to the most optimal image plane is lacking. Both transverse views as well as images aligned with the LV short axis may be used [44, 54, 81]. In our experience, transverse sections improve speed of setup of the study. In this orientation, partial volume effects may cause difficulties in contour detection, particularly at the diaphragmatic level. However, it appears that ventricular volume measurements are less influenced by partial volume effects at the diaphragmatic level than by difficulties in AV valve border detection, which often occur in short-axis images [11]. Partial volume effects occur regardless of the image orientation, and accuracy of ventricular volume measurements has been shown not to be influenced by imaging plane strategy [11]. Therefore, for studies primarily aimed at the RV we tend to use transverse sections.

The importance of LV function in patients who have undergone repair of TOF has become increasingly clear [2, 3, 37, 75, 93]. For studies aimed at biventricular function or the interaction between RV and LV, images aligned with the LV short axis are probably best suited (Fig. 4). The number of studies on ventricular function in TOF in which MRI was used is limited [25, 59, 60, 85]. MRI was used to assess the influence of pulmonary regurgitation on RV size and function in a group of 18 patients aged 16.5 ± 6.5 years (range 8.6 to 30.2) previously discussed [70]. MR-derived RV end diastolic volume index was 138 ± 38 ml/m^2 in those patients with a transannular patch ($n = 8$) and 90 ± 18 ml/m^2 in those without a transannular patch ($n = 10$) ($p < 0.005$) [70]. RV ejection fraction was generally normal in this group of 18 patients (59 ± 8%, range 34–67%), who had a pulmonary regurgitant fraction (regurgitant pulmonary flow volume/forward pulmonary flow volume) of 30 ± 18% [70]. A significant correlation could be established between the amount of pulmonary regurgitation and RV ejection fraction ($r = -0.59$), RV end diastolic volume ($r = 0.72$), and RV end systolic volume ($r = 0.74$) [70]. In a younger group of 19 TOF patients (12 ± 3 years), with larger amounts of pulmonary regurgitation (39 ± 16%), we found RV ejection fraction (54 ± 8%) to be significantly lower than that of an age- and sex-matched control group (66 ± 7%, $p < 0.01$) [59]. This finding confirmed the correlation between the actual amount of pulmonary regurgitation and RV ejection fraction.

With regard to LV function, some studies in patients with residual pulmonary regurgitation after repair of TOF have indicated impaired LV function, whereas others have reported normal LV function in similar patient groups [2, 3, 37, 47, 67, 75]. This discrepancy has not been fully explained. A possible explanation may be that the patient groups under study differed with regard to the amount of pulmonary regurgitation. This could not be assessed without MRI [95]. In two groups of patients in whom pulmonary regurgitation had been quantified with MRI, we noted significant differences in LV function. In a group of children with 39 ± 16% pulmonary regurgitation, LV ejection fraction was 52 ± 10% compared with 68 ± 7% in controls ($p < 0.001$) [59]. In adults with 25 ± 18% pulmonary regurgitation, LV ejection fraction did not differ from normal controls [60]. From these observations, it is suggested that LV function may be preserved with mild pulmonary regurgitation, but it will deteriorate with larger amounts of regurgitation. MRI is an excellent tool for further studies in this field since it is particularly suited for longitudinal studies of patient

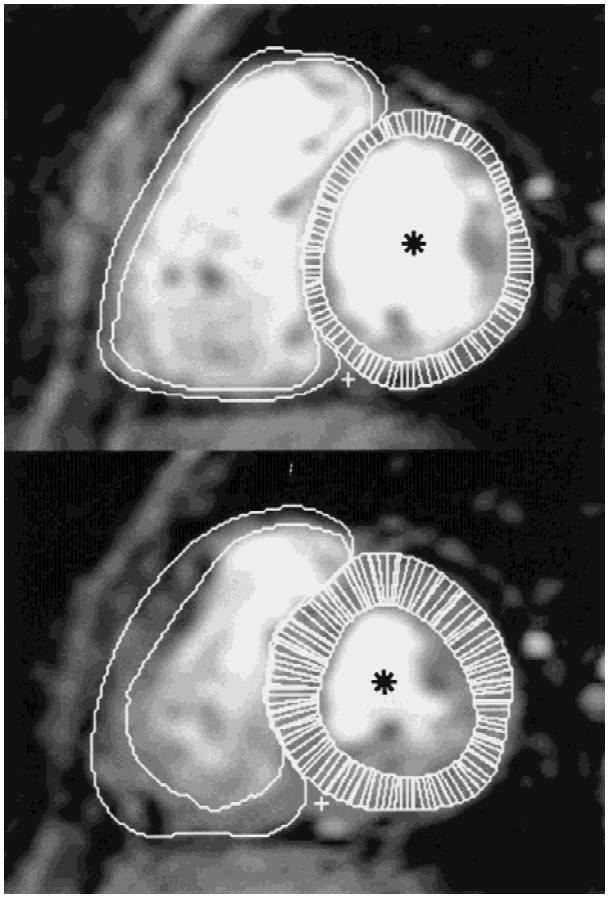

Fig. 4. Gradient-echo image of the heart of a patient operated for tetralogy of Fallot, at midventricular level at end diastole (*top*) and end systole (*bottom*). The endocardial and epicardial borders of the LV and RV are outlined. Ventricular volumes and wall mass are calculated by summation of ventricular cavity and wall areas outlined on a multisection, multiphase image set of a specific time frame multiplied by section thickness (and a specific gravity of 1.05 g/ml for wall mass). Note hypertrophy of RV wall. *, left ventricle

groups. Currently, MRI has to our knowledge not been used for this purpose.

Right Ventricular Diastolic Function

In recent years, diastolic function of the RV has been recognized as an additional important factor in the long-term outcome of TOF [19, 25, 56, 64, 65, 85]. In adults, restriction of RV filling was associated with superior exercise performance [19]. Restrictive RV physiology has also been related to decreased QRS duration, indicating a decreased change of malignant ventricular arrhythmias [20]. An inverse relationship between age at repair and restrictive RV physiology has been documented [56]. Available data are inconclusive on the role of transannular patching in the development of restrictive RV physiology [56, 65]. From the studies on restrictive RV physiology, it may be hypothesized that a myocardial restrictive process, induced by factors related to age at repair, may limit the amount of pulmonary regurgitation and RV dilatation [19, 25]. The inability to quantify the amount of pulmonary regurgitation and RV size has been a major limitation of all echocardiographic studies on RV diastolic function [19, 56, 64, 65]. Other limitations of echocardiography in this setting are that it does not provide reliable measurements of RV wall mass and that diastolic RV function cannot be quantified with echo-Doppler techniques in the presence of inflow from two sources, as occurs with pulmonary regurgitation. These limitations of echocardiography have prevented adequate comparison of the studies on RV diastolic function in TOF [19, 25, 56, 64, 65, 85]. The opportunities to study RV diastolic function with MRI include quantification of tricuspid flow patterns with velocity mapping techniques and reconstruction of RV time–volume curves from tomographic (either spin-echo or gradient-echo) multislice cine MRI [55, 88]. By plotting RV volume of the various time phases of diastole against time, a RV time volume curve may be obtained. From this curve the usual indices of diastolic function may be derived [85, 88]. This is a very time-consuming process. Furthermore, with conventional MR gating techniques, information on the last part of diastole is not provided.

We have reconstructed RV time–volume flow curves that include the last part of diastole by combining tricuspid (Fig. 5) and pulmonary flow (see Fig. 3) volume curves, obtained with velocity mapping MRI with retrograde ECG gating [25] (Figs. 3 and 5). Time–volume curves were obtained by integration of the time–volume change curves (Fig. 6). From these curves indexes of diastolic function were derived (Fig. 6).

This method provides adequate temporal resolution (30 time frames/cardiac cycle) and requires drawing of less complicated contours (which may be performed semiautomatically). This technique may be associated with less inter- and intraobserver variability than tomographic cine MR techniques. Combined with a single-phase, multisection volume measurement, this technique provides most clinically important data on RV function in these patient groups, including RV mass. In a study of 19 children operated for TOF [age (mean ± SD) 12 ± 3 years, operated at 1.5 ± 1 years] and 12 healthy children, we found late diastolic forward pulmonary artery flow to be absent in 6 patients (group I) [25]. In 13 patients (group II) late diastolic forward pulmonary artery flow contributed 1% to 14% to RV stroke volume [25]. Significant differences with controls in group I were increased deceleration time (315 ± 91 msec vs 168 ± 28 msec, $p < 0.001$) and decreased filling fraction (44 ± 11% vs 55 ± 16%, $p = 0.02$) [25]. These data indicate impaired RV relaxation. Significant differences between group II and controls for RV parameters were increased peak early filling rate (378 ± 124 vs 286 ± 112 ml/sec, $p = 0.018$) and increased deceleration time (230 ± 40 msec, $p = 0.03$), which is less marked than in group I), indicating restriction to RV filling [25]. Pulmonary regurgitation, ventricular size, RV wall mass, and ejection fraction did not differ significantly between groups I and II [25]. Exercise function was diminished with restrictive RV physiology (group II; $p < 0.001$ vs controls) [25]. From this study it was concluded that both impaired relaxation and restriction to filling affect diastolic RV function in children with operated TOF and pulmonary regurgitation [25]. Contrary to the findings in adults [19], restrictive RV physiology was associated with decreased exercise function in these children [25]. The relation between abnormal RV diastolic function and decreased exercise performance in children operated for TOF has recently been confirmed in another MRI study [85]. Prospective MRI studies in properly matched groups of TOF patients should allow clarification of some of the discrepancies in the results of various studies on RV diastolic function in TOF.

Ventricular Mass

Left ventricular mass can be assessed accurately with echocardiography. For measurements of RV mass, echocardiography, angiography, and radionuclide techniques have various limitations [46]. Biventricular mass can be assessed in a reproducible and accurate way with MRI [46, 69, 79] (Fig. 4). Lorenz et al. [46] reported results of biventricular wall mass in 75 healthy subjects, age 8 to 55 years. The normal range for RV free wall mass in their study was 26 ± 5 g/m^2, for LV free wall mass 57 ± 8 g/m^2, and for the interventricular septum 30 ± 4 g/m^2.

In TOF intrinsic abnormalities of overall myoarchitecture are present [80]. Several studies have shown that myocardial hypertrophy and fibrosis may persist after surgical repair [53, 79, 82]. Ventricular hypertrophy has

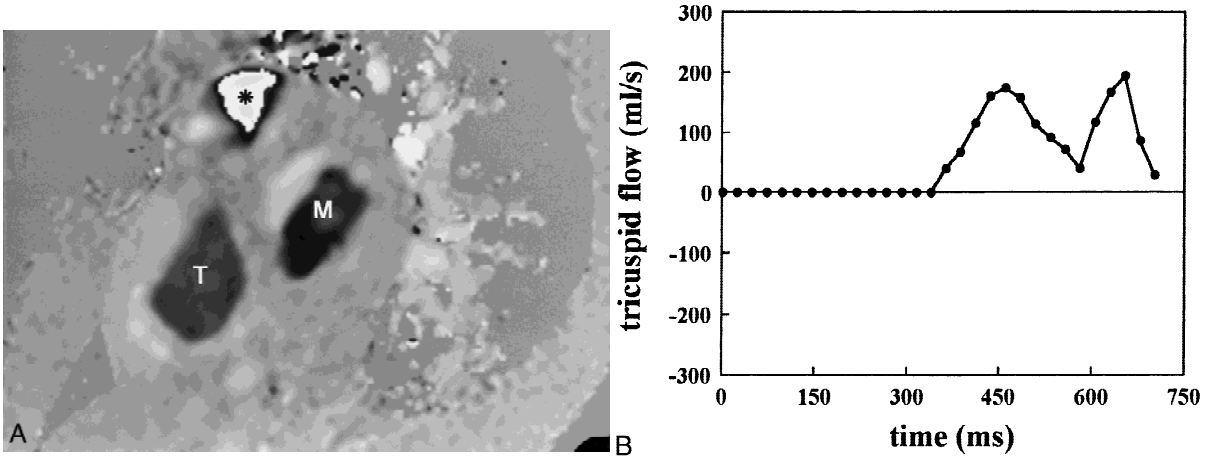

Fig. 5. (A) Velocity map of double-oblique image obtained with the flow-adjusted gradient across the tricuspid valve (*T*) and mitral valve (*M*) of a patient operated for tetralogy of Fallot. Dark signal indicates (early diastolic) flow into the ventricle. Spatial peak and spatial average velocities are obtained from the darkest and average signal intensities across the tricuspid valve orifice, which is manually outlined. Note aliasing in pulmonary artery (*) as a result of high flow velocity with residual pulmonary stenosis. **(B)** Time–volume flow velocity curve of tricuspid valve. Flow velocity–time frame was calculated by multiplying tricuspid orifice area (Fig. 5A; traced manually) with the spatial average flow within this contour.

been associated with the risk of sudden death after repair of TOF [5]. These observations indicate the need for assessment of ventricular mass in the follow-up of operated TOF. As has been discussed, we have used MRI to assess RV mass in children with tetralogy and healthy age- and sex-matched controls [25]. In children operated for TOF, RV wall mass was significantly higher (26 ± 7 g/m^2) than that of healthy children (17 ± 2 g/m^2). These findings could not directly be related to the measurements of ventricular function [25]. Again, MRI is the technique of choice with regard to follow-up studies, which will help to further understand the importance of increased RV mass in these patient groups.

Motion Tracking Techniques

Assessment of 3-D myocardial motion is another application of MRI techniques [50]. Available techniques are MR tagging and velocity-encoding techniques. By inducing magnetization changes in localized tissue areas, MR imaging allows superimposition of tagging grids on conventional MR images. The tagging grid then serves as a reference point in the myocardium, enabling tracking of these reference points during contraction [50]. Velocity-encoding methods using phase encoding of the velocity of transverse magnetization to quantify the dynamics of the tissue [50]. These techniques allow analysis of re-

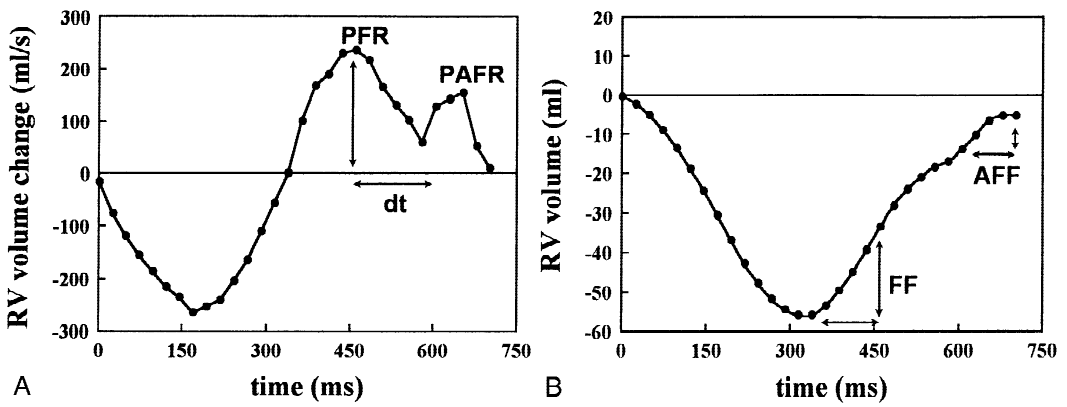

Fig. 6. Right ventricular time–volume change curve (*A*) and right ventricular time–volume curve (*B*) of a Fallot patient. Negative values indicate flow out of the right ventricle (*A*) or decrease in right ventricular volume (*B*). The curve in A was obtained by summation of curves in Figs. 3B and 5B and the curve in B by integration of the curve in A. *AFF,* atrial filling fraction; *dt,* deceleration time; *FF,* filling fraction in first one third of diastole; *PFR,* peak filling rate; *PAFR,* atrial filling fraction; *RV,* right ventricle.

gional strain and wall motion. Currently, MRI tagging techniques have been applied in only a limited number of studies in patients with congenital heart disease, not including TOF [16–18]. These techniques will certainly help increase knowledge of ventricular dynamics in patients with abnormal loading conditions [58].

Conclusions

In clinical practice, both anatomical and functional information may be obtained with MRI in patients who have undergone surgical repair of TOF. This is particularly true for patients in whom transthoracic echocardiography fails to provide the required information. With MRI, the pulmonary artery may be imaged with great detail, often preventing the need for (invasive) x-ray angiography. Quantification of biventricular systolic and diastolic function and wall mass probably allows identification of those patients requiring more detailed (invasive) hemodynamic measurements. In many patients operated for TOF, MRI will allow clinical problem solving in an entirely noninvasive way.

References

1. Beekman RP, Beek FJ, Meijboom EJ (1997) Usefulness of MRI for the pre-operative evaluation of the pulmonary arteries in tetralogy of Fallot. *Magn Reson Imaging 15*:1005–1015
2. Borow KM, Green LH, Castaneda AR, Keane JF (1980) left ventricular function after repair of tetralogy of Fallot and its relationship to age at surgery. *Circulation 61*:1150–1158
3. Bove EL, Byrum CJ, Thomas FD, et al. (1983) The influence of pulmonary insufficiency on ventricular function following repair of tetralogy of Fallot. *J Thorac Cardiovasc Surg 85*:691–696
4. Boxt LM, Katz J, Kolb T, Czegledy FP, Barst RB (1992) Direct quantitation of right and left ventricular volumes with nuclear magnetic resonance imaging in patients with primary pulmonary hypertension. *J Am Coll Cardiol 19*:1508–1515
5. Bricker JT (1995) Sudden death and tetralogy of Fallot. Risks, markers, and causes. *Circulation 92*:162–163
6. Buller VGM, van der Geest RJ, Kool MD, et al. (1997) Assessment of regional left ventricular wall parameters from short axis magnetic resonance imaging using a three dimensional extension to the improved centerline method. *Invest Radiol 32*:529–539
7. Caputo GR, Kondo C, Masui T, et al. (1991) Right and left lung perfusion: in vitro and in vivo validation with oblique-angle, velocity-encoded cine MR imaging. *Radiology 180*:693–698
8. Carvalho JS, Shinebourne EA, Busst C, Rigby ML, Redington AN (1992) Exercise capacity after complete repair of tetralogy of Fallot: deleterious effects of residual pulmonary regurgitation. *Br Heart J 67*:470–473
9. Chaturvedi RR, Kilner PJ, White PA, et al. (1997) Increased airway pressure and simulated branch pulmonary artery stenosis increase pulmonary regurgitation after repair of tetralogy of Fallot. Real-time analysis with a conductance catheter technique. *Circulation 95*:643–649
10. Chrispin A, Small P, Rutter N, et al. (1986) Transectional echo planar imaging of the heart in cyanotic congenital heart disease. *Pediatr Radiol 16*:293–297
11. Cranney GB, Lotan CS, Dean L, et al (1990) Left ventricular volume measurement using cardiac axis nuclear magnetic resonance imaging. Validation by calibrated ventricular angiography. *Circulation 82*:154–163
12. Duerinckx AJ, Wexler L, Banerjee A, et al. (1994) Postoperative evaluation of pulmonary arteries in congenital heart surgery by magnetic resonance imaging: comparison with echocardiography. *Am Heart J 128*:1139–1146
13. Firmin DN, Nayler GL, Klipstein RH, et al. (1987) In vivo validation of MR velocity imaging. *J Comput Assist Tomogr 11*:751–756
14. Fisher MR, Lipton MJ, Higgins CB (1985) Magnetic resonance imaging and computed tomography in congenital heart disease. *Semin Roentgenol 20*:272–282
15. Fletcher BD, Jacobstein MD, Nelson AD, Riemenschneider TA, Alfidi RJ (1984) Gated magnetic resonance imaging of congenital cardiac malformations. *Radiology 150*:137–140
16. Fogel MA, Gupta KB, Weinberg PM, Hoffman EA (1995) Regional wall motion and strain analysis across stages of Fontan reconstruction by magnetic resonance tagging. *Am J Physiol 269*:H1132–1152
17. Fogel MA, Weinberg PM, Fellows KE, Hoffman EA (1995) A study in ventricular–ventricular interaction. Single right ventricles compared with systemic right ventricles in a dual-chamber circulation. *Circulation 92*:219–230
18. Fogel MA, Weinberg PM, Gupta KB, et al. (1998) Mechanics of the single left ventricle: a study in ventricular–ventricular interaction II. *Circulation 98*:330–338
19. Gatzoulis MA, Clark AL, Cullen S, Newman CGH, Redington AN (1995) Right ventricular diastolic function 15 to 35 years after repair of tetralogy of Fallot. Restrictive physiology predicts superior exercise performance. *Circulation 91*:1775–1781
20. Gatzoulis MA, Till JA, Somerville J, Redington AN (1995) Mechanoelectrical interaction in tetralogy of Fallot. QRS prolongation relates to right ventricular size and predicts malignant ventricular arrhythmias and sudden death. *Circulation 92*:231–237
21. Graham TP Jr (1991) Ventricular performance in congenital heart disease. *Circulation 84*:2259–2274
22. Hartnell GG, Notarianni M (1998) MRI and echocardiography: how do they compare in adults? *Semin Roentgenol 33*:252–261
23. Hawkes RC, Holland GN, Moore WS, Roebuck EJ, Worthington BS (1981) Nuclear magnetic resonance (NMR) tomography of the normal heart. *J Comput Assist Tomogr 5*:605–612
24. Helbing WA, Bosch HG, Maliepaard C, et al. (1995) Comparison of echocardiographic methods with magnetic resonance imaging for assessment of right ventricular function in children. *Am J Cardiol 76*:589–594
25. Helbing WA, Niezen RA, LeCessie S, et al. (1996) Right ventricular diastolic function in children with pulmonary regurgitation after repair of tetralogy of Fallot: volumetric evaluation by magnetic resonance velocity mapping. *J Am Coll Cardiol 28*:1827–1835
26. Helbing WA, Rebergen SA, Maliepaard C, et al. (1995) Quantification of right ventricular function with magnetic resonance imaging in children with normal hearts and with congenital heart disease. *Am Heart J 130*:828–837
27. Herfkens RJ, Higgins CB, Hricak H, et al. (1983) Nuclear magnetic resonance imaging of the cardiovascular system: normal and pathologic findings. *Radiology 147*:749–759
28. Hernandez RJ (1996) Cardiovascular MR imaging of children. *Magn Reson Imaging Clin North Am 4*:615–636
29. Higgins CB, Byrd BF, Farmer DW, et al. (1984) Magnetic reso-

nance imaging in patients with congenital heart disease. *Circulation 70*:851–860
30. Hirsch R, Kilner PJ, Connelly MS, et al. (1994) Diagnosis in adolescents and adults with congenital heart disease. Prospective assessment of individual and combined roles of magnetic resonance imaging and transesophageal echocardiography. *Circulation 90*:2937–2951
31. Hoffman JI (1995) Incidence of congenital heart disease: I. postnatal incidence. *Pediatr Cardiol 16*:103–113
32. Horneffer PJ, Zakha KG, Rowe SA, et al. (1990) Long-term results of total repair of tetralogy of Fallot in childhood. *Ann Thorac Surg 50*:179–185
33. Ilbawi MN, Idriss FS, DeLeon SY, et al. (1987) Factors that exaggerate the deleterious effects of pulmonary insufficiency in the right ventricle after tetralogy repair. *J Thorac Cardiovasc Surg 93*:36–44
34. Jiang L, Siu SC, Handschumacher MD, et al. (1994) Three-dimensional echocardiography. In vivo validation for right ventricular volume and function. *Circulation 89*:2342–2350
35. Kauczor H-U (1998) Contrast-enhanced magnetic resonance angiography of the pulmonary vasculature. A review. *Invest Radiol 9*:606–617
36. Kaufman L, Crooks LE, Higgins CB (1985) Magnetic resonance imaging of the cardiovascular system. *Am Heart J 109*:136–152
37. Kavey RE, Thomas FD, Byrum CJ, et al. (1984) Ventricular arrhythmias and biventricular dysfunction after repair of tetralogy of Fallot. *J Am Coll Cardiol 4*:126–131
38. Kersting-Sommerhoff BA, Diethelm L, Teitel DF, et al. (1989) Magnetic resonance imaging of congenital heart disease: sensitivity and specificity using receiver operating characteristic curve analysis. *Am Heart J 118*:155–161
39. Kirklin JK, Kirklin JW, Blackstone EH, Milano A, Pacifico AD (1989) Effect of transannular patching on outcome after repair of tetralogy of Fallot. *Ann Thorac Surg 48*:783–791
40. Lange PE, Onnasch DGW, Bernard A, Heintzen PH (1982) Left and right ventricular adaptation to right ventricular volume overload before and after surgical repair of tetralogy of Fallot. *Am J Cardiol 50*:786–794
41. Lange PE, Seiffert PA, Pices F, et al. (1985) Value of image enhancement and injection of contrast medium for right ventricular volume determination by two-dimensional echocardiography in congenital heart disease. *Am J Cardiol 55*:152–157
42. Leung DA, Debatin JF (1997) Three-dimensional contrast-enhanced magnetic resonance angiography of the thoracic vasculature. *Eur Radiol 7*:981–987
43. Levine RA, Gibson TC, Aretz T, et al. (1984) Echocardiographic measurement of right ventricular volume. *Circulation 69*:497–505
44. Lillehei CW, Cohen M, Warden HE, et al. (1955) Direct vision intracardiac surgical correction of the tetralogy of Fallot, pentalogy of Fallot and pulmonary atresia defects: report of the first ten cases. *Ann Surg 142*:418–445
45. Longmore DB, Underwood SR, Hounsfield GN, et al. (1985) Dimensional accuracy of magnetic resonance imaging in studies of the heart. *Lancet 1*:1360–1362
46. Lorenz CH, Walker ES, Morgan VL, Klein SS, Graham TP Jr (1999) Normal human right and left ventricular mass, systolic function, and gender differences by cine magnetic resonance imaging. *J Cardiovasc Magn Res 1*:7–21
47. Marie PY, Marcon F, Brunotte F, et al. (1992) Right ventricular overload and induced sustained ventricular tachycardia in operatively "repaired" tetralogy of Fallot. *Am J Cardiol 69*:785–789
48. Marx GR, Geve T (1998) MRI and echocardiography in children: how do they compare? *Semin Roentgenol 3*:281–292
49. Marx GR, Hicks RW, Allen HD, Goldberg SJ (1988) Non-invasive assessment of hemodynamic responses to exercise in pulmonary regurgitation after operations to correct pulmonary outflow obstruction. *Am J Cardiol 61*:595–601
50. McVeigh ER (1996) MRI of myocardial function: motion tracking techniques. *Magn Reson Imaging 14*:137–150
51. Meier D, Maier S, Bosiger P (1988) Quantitative flow measurements on phantoms and on blood vessels with MR. *Magn Reson Med 8*:25–34
52. Mirowitz SA, Gutierrez FR, Canter CE, Vannier MW (1989) Tetralogy of Fallot: MR findings. *Radiology 171*:207–212
53. Mitsuno M, Nakano S, Shimazaki Y, et al. (1993) Fate of right ventricular hypertrophy in tetralogy of Fallot after corrective surgery. *Am J Cardiol 72*:694–698
54. Møgelvang J, Stubgaard M, Thomsen C, Henriksen O (1988) Evaluation of right ventricular volumes measured by magnetic resonance imaging. *Eur Heart J 9*:529–533
55. Mostbeck GH, Hartiala JJ, Foster E, et al. (1993) Right ventricular diastolic filling: evaluation with velocity-encoded cine MRI. *J Comput Assist Tomogr 17*:245–252
56. Munkhammar P, Cullen S, Jögi P, et al. (1998) Early age at repair prevents right ventricular (RV) physiology after surgery for tetralogy of Fallot (TOF). Diastolic RV function after TOF repair in infancy. *J Am Coll Cardiol 32*:1083–1087
57. Murphy JG, Gersh BJ, Mair DD, et al. (1993) Long-term outcome in patients undergoing surgical repair of tetralogy of Fallot. *N Engl J Med 329*:593–599
58. Naito H, Arisawa J, Harada K, et al. (1995) Assessment of right ventricular regional contraction and comparison with the left ventricle in normal humans: a cine magnetic resonance study with presaturation myocardial tagging. *Br Heart J 74*:186–191
59. Niezen RA, Helbing WA, van der Geest RJ, van der Wall EE, de Roos A (1996) Biventricular systolic function and mass studied with magnetic resonance imaging in children with pulmonary regurgitation after correction for tetralogy of Fallot. *Radiology 201*: 135–140
60. Niezen RA, Helbing WA, van der Wall EE, et al. (1999) Left ventricular function in adults with mild pulmonary regurgitation. *Heart* (in press)
61. Ninomiya K, Duncan WJ, Cook DH, Olley PM, Rowe RD (1981) Right ventricular ejection fraction and volumes after Mustard repair: correlation of two dimensional echocardiograms and cineangiograms. *Am J Cardiol 48*:317–324
62. Niwa K, Uchishiba M, Aotsuka H, et al. (1996) Measurement of ventricular volumes by cine magnetic resonance imaging in complex congenital heart disease with morphologically abnormal ventricles. *Am Heart J 131*:567–575
63. Nollert G, Fischlein T, Bouterwerk S, et al. (1997) Long-term survival in patients with repair of tetralogy of Fallot: 36-year follow-up of 490 survivors of the first year after surgical repair. *J Am Coll Cardiol 30*:1374–1383
64. Nørgard G, Gatzoulis MA, Josen M, Cullen S, Redington AN (1998) Does restrictive right ventricular physiology in the early postoperative period predict subsequent right ventricular restriction after repair of tetralogy of Fallot? *Heart 79*:481–484
65. Nørgard G, Gatzoulis MA, Moraes F, et al. (1996) Relationship between type of outflow tract repair and postoperative right ventricular diastolic physiology in tetralogy of Fallot. Implications for long-term outcome. *Circulation 94*:3276–3280
66. Oldershaw P (1992) Assessment of right ventricular function and its role in clinical practice. *Br Heart J 68*:12–15
67. Oku H, Shirontani H, Sunakawa A, Yokoyama T (1986) Postoperative long-term results in total correction of tetralogy of Fallot: hemodynamics and cardiac function. *Ann Thorac Surg 41*:413–418
68. Papavassiliou DP, Parks WJ, Hopkins KL, Fyfe DA (1998) Three-

dimensional echocardiographic measurement of right ventricular volume in children with congenital heart disease validated by magnetic resonance imaging. *J Am Soc Echocardiogr 11*:770–777
69. Pattynama PM, Lamb HJ, Van der Velde EA, et al. (1995) Reproducibility of MRI-derived measurements of right ventricular volumes and myocardial mass. *Magn Reson Imaging 13*:53–63
70. Rebergen SA, Chin JG, Ottenkamp J, van der Wall EE, de Roos A (1993) Pulmonary regurgitation in the late postoperative follow-up of tetralogy of Fallot. Volumetric quantitation by nuclear magnetic resonance velocity mapping. *Circulation 88*:2257–2266
71. Rebergen SA, Ottenkamp J, Doornbos J, et al. (1993) Postoperative pulmonary flow dynamics after Fontan surgery: assessment with nuclear magnetic resonance velocity mapping. *J Am Coll Cardiol 21*:123–131
72. Rebergen SA, van der Wall EE, Doornbos J, de Roos A (1993) Magnetic resonance measurement of velocity and flow: technique, validation, and cardiovascular applications. *Am Heart J 126*:1439–1456
73. Reddy VM, Liddicoat JR, McElhinney DB, et al. (1995) Routine primary repair of tetralogy of Fallot in neonates and infants less than three months of age. *Ann Thorac Surg 60*:S592–S596
74. Redington AN, Oldershaw PJ, Shinebourne EA, Rigby ML (1988) A new technique for the assessment of pulmonary regurgitation and its application to the assessment of right ventricular function before and after repair of tetralogy of Fallot. *Br Heart J 60*:57–65
75. Reduto LA, Berger HJ, Johnstone DE, et al. (1980) Radionuclide assessment of right and left ventricular exercise reserve after total correction of tetralogy of Fallot. *Am J Cardiol 45*:1013–1018
76. Rowe SA, Zahka KG, Manolio TA, Horneffer PJ, Kidd L (1991) Lung function and pulmonary regurgitation limit exercise capacity in postoperative tetralogy of Fallot. *J Am Coll Cardiol 17*:461–466
77. Rosenthal A (1993) Adults with tetralogy of Fallot—repaired, yes; cured, no (editorial). *N Engl J Med 329*:655–656
78. Ryan T, Petrovic O, Dillon JC, et al. (1985) An echocardiographic index for separation of right ventricular volume and pressure overload. *J Am Coll Cardiol 5*:918–927
79. Sakuma H, Fujita N, Foo TK, et al. (1993) Evaluation of left ventricular volume and mass with breath-hold cine MR imaging. *Radiology 188*:377–380
80. Sanchez-Quintana D, Anderson RH, Ho SY (1996) Ventricular myoarchitecture in tetralogy of Fallot. *Heart 76*:280–286
81. Sechtem U, Pflugfelder PW, Gould RG, Cassidy MM, Higgins CB (1987) Measurement of right and left ventricular volumes in healthy individuals with cine MR imaging. *Radiology 163*:697–702.
82. Seliem MA, Wu Y-T, Glenwright K (1995) Relation between age at surgery and regression of right ventricular hypertrophy in tetralogy of Fallot. *Pediatr Cardiol 16*:53–55
83. Silverman NH, Hudson S (1983) Evaluation of right ventricular volume and ejection fraction in children by two-dimensional echocardiography. *Pediatr Cardiol 4*:197–203
84. Simpson IA, Maciel BC, Moises V, et al. (1993) Cine magnetic resonance imaging and color Doppler flow mapping displays of flow velocity, spatial acceleration, and jet formation: a comparative in vitro study. *Am Heart J 126*:1165–1174
85. Singh GK, Greenberg SB, Yap YS, et al. (1998) Right ventricular function and exercise performance late after primary repair of tetralogy of Fallot with the transannular patch in infancy. *Am J Cardiol 81*:1378–1382
86. Steiner P, McKinnon GC, Romanovski B, et al. (1997) Contrast-enhanced, ultrafast 3D pulmonary MR angiography in a single breath-hold: initial assessment of imaging performance. *J Magn Reson Imaging 7*:177–182
87. Strouse PJ, Hernandez RJ, Beekman RH (1996) Assessment of central pulmonary arteries in patients with obstructive lesions of the right ventricle: comparison of MR imaging and cineangiography. *Am J Roentgenol 167*:1175–1183
88. Suzuki J-I, Chang J-M, Caputo GR, Higgins CB (1991) Evaluation of right ventricular early diastolic filling by cine nuclear magnetic resonance imaging in patients with hypertrophic cardiomyopathy. *J Am Coll Cardiol 18*:120–126
89. Vannier MW, Gutierrez FR, Laschinger JC, et al. (1988) Three-dimensional magnetic resonance imaging of congenital heart disease. *Radiographics 8*:857–871
90. Vick GW 3rd, Rokey R, Huhta JC, Mulvagh SL, Johnston DL (1990) Nuclear magnetic resonance imaging of the pulmonary arteries, subpulmonary region, and aortopulmonary shunts: a comparative study with two-dimensional echocardiography and angiography. *Am Heart J 119*:1103–1110
91. Vick GW 3rd, Wendt RE 3rd, Rokey R (1994) Comparison of gradient echo with spin echo magnetic resonance imaging and echocardiography in the evaluation of major aortopulmonary collateral arteries. *Am Heart J 127*:1341–1347
92. Vogel M, Gutberlet M, Dittrich S, Hosten N, Lange PE (1997) Comparison of transthoracic three-dimensional echocardiography with magnetic resonance imaging in the assessment of right ventricular volume and mass. *Heart 78*:127–130
93. Waien SA, Liu PP, Ross BL, et al. (1992) Serial follow-up of adults with repaired tetralogy of Fallot. *J Am Coll Cardiol 20*:295–300
94. Wessel HU, Cunningham WJ, Paul MH, et al. (1980) Exercise performance in tetralogy of Fallot after intracardiac repair. *J Thorac Cardiovasc Surg 80*:582–593
95. Wessel HU, Paul MH (1999) Exercise studies in tetralogy of Fallot: a review. *Pediatr Cardiol 20*:39–47